Hi-rep. Counter-Illumination Fast Ignition Scheme Fusion*)

Yoneyoshi KITAGAWA, Yoshitaka MORI, Osamu KOMEDA, Katsuhiro ISHII, Ryohei HANAYAMA, Kazuhisa FUJITA, Shin-ichiro OKIHARA, Takashi SEKINE[1)], Nakahiro SATO[1)], Takashi KURITA[1)], Toshiyuki KAWASHIMA[1)], Hirofumi KAN[1)], Naoki NAKAMURA[2)], Takuya KONDO[2)], Manabu FUJINE[2)], Hirozumi AZUMA[3)], Tomoyoshi MOTOHIRO[3)], Tatsumi HIOKI[3)], Mitsutaka KAKENO[3)], Yasuhiko NISHIMURA[4)], Atsushi SUNAHARA[5)] and Yasuhiko SENTOKU[6)]

The Graduate School for the Creation of New Photonics Industries, 1955-1 Kurematsu-cho, Nishi-ku, Hamamatsu, Shizuoka 431-1202, Japan

[1)]*Development Bureau, Hamamatsu Photonics K.K., 1820 Kurematsu-cho, Nishi-ku, Hamamatsu 431-1202, Japan*

[2)]*Advanced Material Engineering Div., TOYOTA Motor Corporation, 1200 Mishuku, Susono, Shizuoka 410-1193, Japan*

[3)]*TOYOTA Central Research and Development Laboratories, Inc., 41-1 Yokomichi, Nagakute 480-1192, Japan*

[4)]*Toyota Technical Development Corp., 1-21 Imae, Hanamoto-cho, Toyota 470-0334, Japan*

[5)]*Institute for Laser Technology, 1-8-4 Utsubo-honmachi, Nishi-ku, Osaka 550-0004, Japan*

[6)]*Department of Physics, University of Nevada, Reno 1664 N VIRGINIA ST Reno, NV 89557, USA*

(Received 22 May 2012 / Accepted 5 September 2012)

A table-top fusion experiment is performed. A 4 J/0.4-ns output of an LD-pumped high-rep. laser HAMA is divided into the imploding and heating beams, which are illuminated on double deuterated polystyrene foils separated by 100 μm. Hot electrons produced by the heating pulses heat the imploded core, emitting X-ray radiations >20 eV and yielding some 10^3 thermal neutrons. The result shows an important step toward developing the fast-ignition scheme fusion plant.

© *2013 The Japan Society of Plasma Science and Nuclear Fusion Research*

Keywords: laser-diode(LD)-pumped laser, ICF roadmap, counter-illumination and fast-ignition scheme fusion, DD fusion

DOI: 10.1585/pfr.8.3404047

1. Introduction

Figure 1 shows the key issues together with the roadmap for achieving an inertial confinement fusion (ICF) power plant [1]. The National Ignition Facility (NIF) is to achieve ignition and burning of fuel. Although this represents an important milestone toward developing an fusion power plant, the main stage for achieving inertial fusion energy does not use single-shot mode, but rather it uses repetitive-shot mode. The main path to the fusion energy is shown on the central row. A lot of works are necessary to realize a power plant [2]. One key issue is the development of a high-repetition-rate, high-efficiency laser with output energies of the order of kilojoules or greater. Another is fuel fabrication and high-repetition fuel injection. In addition, power plant technology, such as an innovative wall materials, will need to be developed.

We divide the roadmap for achieving a fusion plant into three phases. The zeroth phase involves developing 1-kJ drivers perform engineering tests and to produce neutrons. No fuel compression is considered. The first phase is to develop a breakeven machine that uses a 100-kJ driver. Here the fuel is compressed to 100 × the solid density or more. The second phase is to demonstrate a commercial reactor. The fuel may be compressed to around 500 ×. We have developed an LD-pumped laser system with a repetition rate of 10 Hz. This repetition rate is high enough for this stage. We are in the zeroth phase, as indicated

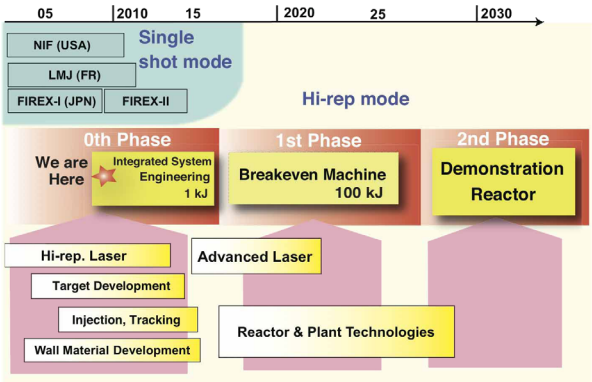

Fig. 1 Key issues and paths to an ICF power plant. Upper left region represents current experiments in single-shot mode. Other regions indicate the main path using repetitive-shot mode toward the fusion power plant. Yellow boxes indicate problems that need to be resolved.

author's e-mail: kitagawa@gpi.ac.jp

*) This article is based on the presentation at the Conference on Inertial Fusion Energy '12.

© 2013 The Japan Society of Plasma Science and Nuclear Fusion Research

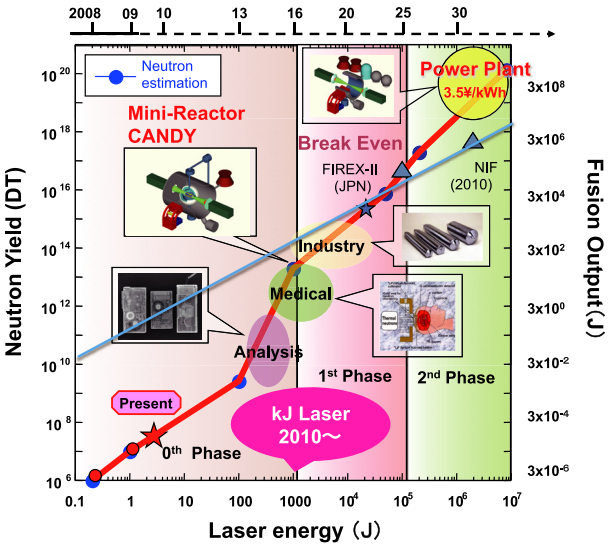

Fig. 2 Neutron yield versus Input laser energy: 0th (0.1 ∼ 1 kJ laser, 1 × compression), 1st (1 ∼ 100 kJ, 100 × compression) and 2nd phase (100 kJ ∼ 10 MJ laser, 100 ∼ 500 × compression).

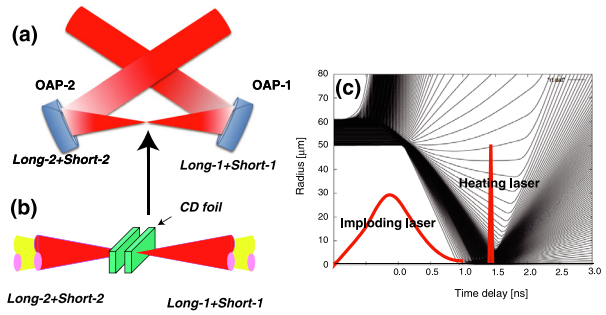

Fig. 3 (a) Counter-illumination scheme and (b) Double foil CD target. Imploding beams (Long beam-1,-2: red) are followed by heating beams (Short beam-1,-2: yellow). (c) STAR 1D hydrodynamic flowchart. The heating beam is delayed between 0.3 and 2.0 ns from the imploding beam peak.

by the star in Fig. 1. Figure 2 plots the neutron yield and the fusion gain versus the input laser energy. The implosion and heating beams are coaxially aligned. The input laser energy is divided 50% to implosion and 50% to fast-heating. The zeroth phase does not provide any fuel compression, but a fuel heating. 100 × compression is considered for the 2nd phase and 100 ∼ 500 × for the 3rd. The zeroth phase output will be an unified Mini-Reactor CANDY, a concept of kJ fast-ignition scheme unified machine, as shown in Fig. 2. The second phase uses the counter-illumination Fast Ignition scheme, where a unit module system of 1.8 MJ laser energy yields the thermal power gain of 200, when the DT bullet fuel is compressed to 500 × the solid density each 0.1 second. A power plant has 4 modules of reactor. The fast-ignition is a very useful scheme for the ICF.

We have started the high-repetition-rate table-top fusion experiment in the counterillumination and fast-ignition scheme (partially reported in [3]) to demonstrate the scheme adequate for the power plant. Here we show that the hot electrons deposit their energy to the peripheral plasma and they reach the core plasma to emit X-ray radiations. Once heated, the core plasma maintains a few hundred electronvolts of temperature as long as the core stagnates. The future plant design will have the counterillumination and fast-ignition scheme.

2. Highly-Repetitive Table-Top Experiment

An LD-pumped high-repetition-rate HAMA laser consists of a seed beam supplier laser "BEAT" and a pump laser "KURE-I". "BEAT" is a Ti:sapphire optical parametric chirped pulse amplification system [4, 5]. KURE-I is an LD-pumped Nd:glass laser system (Hamamatsu Photonics Product), which pumps a Ti:sapphire crystal to amplify the seed beam from "BEAT".

The amplified chirped 3.6 J-800 nm in the 0.4-ns pulse is divided into two beams, one for imploding and another for heating the imploded core. The imploding beam is divided into two beams (Long beam-1 and Long beam-2) and is transported using different paths to the target chamber. The remaining beam is time-delayed and pulse-compressed to a 110-fs Gaussian beam by two pairs of gold-coated plane gratings. This beam is then divided into two heating beams (Short beam-1 and Short beam-2). Short beam-1 is co-aligned to Long beam-1 and Short beam-2 to Long beam-2, respectively. A cross-beam divider stage enables us to coalign the four beams to counter-illuminate both sides of a target. The beam energy is 0.55 J for a long beam and 0.48 J for a short one. The beam diameter is 60 mm.

Using a pair of off-axial 7.6-cm-diameter dielectric-coated mirror (OAP), we counter-focused the beams, such that Long beam-1 and Short beam-1 are focused from the right-hand direction of the target and Long beam-2 and Short beam-2 approach from the left-hand side as shown in Fig. 3 (a). All the beams are p-polarized on the target.

The target consists of two parallel 2-mm square plain foils. The foil is made of deuterated polystyrene ($(C_8D_8)_n$ and is 11 μm thick, supported with 100-μm-thick stainless steel. The separation (gap) between the foils is 100 μm. We set the focal position of the beams at the center between the double foils. The focal spot size w_0 is 32 μm. The intensities are $5.9 \pm 0.5 \times 10^{13}$ and $1.9 \pm 0.3 \times 10^{17}$ [W/cm^2], respectively.

A one-dimensional hydrodynamic code STAR [6] predicted that for 11-μm-thick foils with 100-μm gap, the target rear surfaces meet each other 1.4 ns after the imploding beam peak.

A part of the pulse-compressed beam is converted to

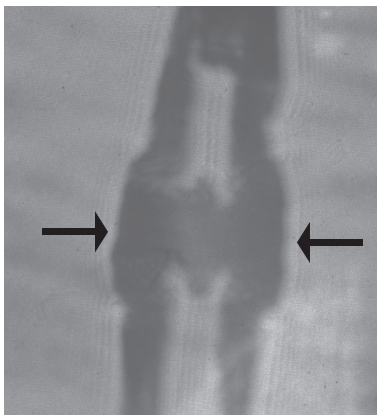

Fig. 4 2ω 100-fs probe captures the double foil image at the moment occurring 1.3 ns after the peak of the imploding beam. A stainless steel supports the double foils. The probe is synchronized with the heating beam. The target is tilted at 1.3° to the probe. ICCD camera is gated at 20 ns.

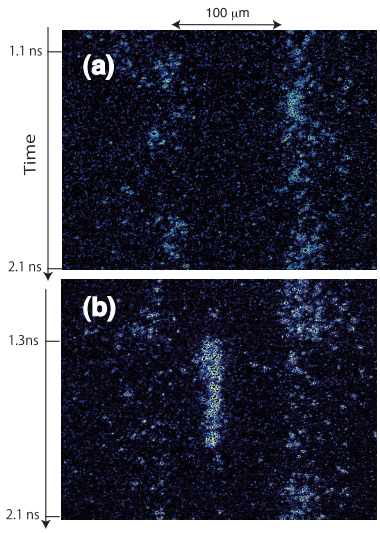

Fig. 5 X-ray streak image of the imploding-heating foils (a) at 1.1-ns delay, no core emission is seen. (b) At 1.3-ns delay, the core is heated. The Au cathode detects emissions not less than 20 eV.

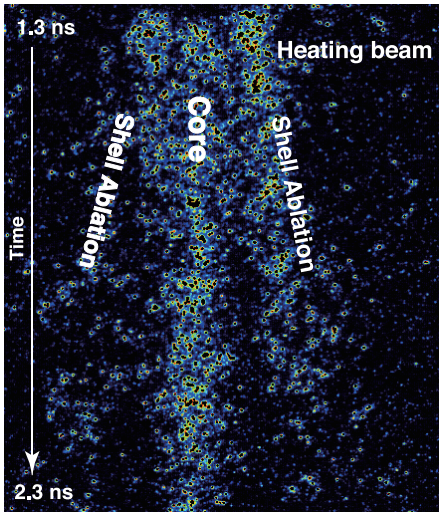

Fig. 6 X-ray core-emissions and their tails at the same condition as in Fig. 5 (b), without the stainless support.

the second harmonics (400-nm wavelength) to probe the collision between two counter-injected plasmas. The probe captures shots of the double foil shadows, just when the compressed core is formed, as in Fig. 4. The probe cutoff density n_c is 6×10^{21} cm^{-3}. The collecting lens with numerical aperture of 7.18 takes an image of the core shadow, whose boundary density is 0.1 n_c. Figure takes 1.3 ns after the compression beam peak and marks the instance of the heating beam illumination. At this time the imploding beams are no longer present. The probe axis is perpendicular to the main beam axis. The plasma image is relayed through an interference filter (394±15 nm) to an ICCD camera that is open for 20 ns. The foil thickness is 11 μm and the gap separation is 100 μm. Since the target is tilted at 1.3°, the foil shadow is observed to be 45 μm thick, not 11 μm thick. At this time, the formed core expands radially.

An X-ray streak camera (Hamamatsu Photonics C4575-03) is used to capture the emissions related to the implosion and heating of the double foils. The 50-μm slit determined the spatial resolution to be 54 μm. The observation is normal to the laser axis and tilted at 1.3° to the target surface. The image is magnified 7.0 times. We used a full-window range of 1.1 ns. The 30-nm Au-coated 100-nm-parylene-N cathode detects photons in the region from 20 eV to 5 keV.

Figure 5 (a) shows the image for the heating beam of a 1.1-ns delay. We see only the emissions due to the initial foil ablations. No core emission is shown. At a 1.3-ns delay, it is seen, as in Fig. 5 (b). The delay agrees with the maximum compression time, predicted by STAR 1D. If no heating beams are illuminated around this time, we observed neither core emissions, nor peripheral emissions. Note that since the stainless support masks the areas between the center and the initial foils, which makes dark grooves between the core emission and the peripheral foil ones.

To make the core emission clear, we removed the stainless support, which is shown in Fig. 6. The figure is the same parameter shot as that in Fig. 5 (b). The heating beams give three bright circular spots at the top and the following central and two side emission tails.

The central emission spot is delayed by 50 ps from the side emission spots and is much strong, which seems to say that the hot electrons generated at the ablation surfaces are transported to the core and heat it up within 50 ps. The hydodynamic thermal transportation will take a longer time. STAR 1D suggests that the side (Shell Ablation) emis-

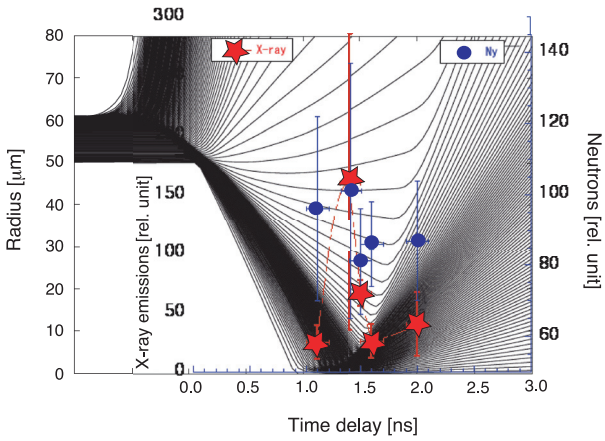

Fig. 7 Diamond: X-ray core-emissions versus the heating beam delay on radius-time diagram. The vertical error bar is the shot-to-shot deviation (standard error) for every 10 shots. Dot: DD thermal neutron time of flight signal from ND3. The error bar is 1σ.

sions are between the cutoff and the ablation surfaces and the central emission is at the imploded core. Although it seems that the side emissions close to the ablation surface are peeled off as time passes, the core stagnates and emits X-rays for 300 ps full-width half maximum (FWHM) or more. These features are observed only when the heating beams are between 1.1 and 2.0 ns.

Figure 7 plotted X-ray core-emissions and DD thermal neutron yield versus the heating beam delay, showing that the imploded cold core is heated by the heating beam to emit X-ray radiations, which is similar to the PW laser results [7]. The vertical error bar is the shot-to-shot deviation (standard error) for every 10 shots. A neutron detector ND3 is a 6-inch plastic scintillator (NE102, 15 cm in diameter and 6 cm in length) coupled to a 2-inch photomultiplier (H7195) located 1.43 m from the target normal to the laser axis [4]. After accumulating each 10 shots, we have filtered the low frequency noises less than 150 MHz out through a Fast Fourier Transform filter, which shows a small peak around 1.4 ns as in Fig. 7. At 1.4 ns, the neutron yield was around 1000, close to that estimated when 30% the laser energy is converted to the core internal one. Since the simulation suggests the core density is compressed to $2\times$ the solid CD density of 1.1 g/cm^3 at least, then the deuteron density will be $n_D = 9\times10^{22}$ cm^{-3}. Assuming the Z number of Carbon is ~ 4, the plasma density in the core will be $n_p = 6\times10^{23}$ cm^{-3}. If 30% of the heating beams energy is absorbed at the cutoff region and is transported into the 30 μm diameter core, and supposed the all particles in the core have the same temperature, then it will be 300 eV. This temperature can yield the neutrons N_y in τ of 300 ps stagnation period as $N_y = n_D^2/4(\sigma v_{th})V\tau \sim 2000$, where $(\sigma v_{th}) = 3.5\times10^{-25}$ cm^3/s and V is the core volume.

Using the electron density profile at the maximum compression calculated by STAR 1D, the 1D PIC (PICLS1d) [8] was performed to study fast electron transport and energy deposition in the imploded plasmas. The preimploded plasmas are initially consisting of carbon and deuteron ions. The carbon (deuteron) ions are ionized at $Z = 2(1)$. They are ionized to a higher charge state through heating. The heating beam with a duration of 100 fs and a peak intensity of 2×10^{17} W/cm^2 is incident from the boundary, which is an absorbing boundary for particles and electromagnetic waves. The absorption of the laser energy is 33.8%, which was small due to the 1D restriction. So that this PIC simulation underestimated the heating performance, more than the experiment suggested. Two groups of hot electrons with 50 and 200 keV in quasi-Maxwellian distributions are produced by the short pulse. The lower energy group contains ponderomotive electrons, which carry most of the absorbed energy. These electrons slow down and deposit energy via collisions. Higher energy electrons are produced below the critical density via plasma waves excitation. These energetic electrons are transported through the imploded plasma and are scattered by the ions. The electron bulk temperature below $\sim 20n_c$ is greater than 100 eV. The core region is also heated up diffusively to ~40 eV electron temperature at 4 ps. At this time the plasma is not thermally equilibrated, and the ion temperature is slightly over 20 eV. So far the simulation does not agree with the experiment. The optimization of the heating laser to achieve the efficient core heating is planned for a future study.

3. Conclusion

We have started the high-repetition-rate table-top fusion experiment in the counterillumination and fast-ignition scheme to demonstrate the scheme adequate for the power plant. The hot electrons reach the core plasma to emit X-ray radiations. Once heated, the core plasma maintains a temperature of more than few tens electron-volts as long as the core stagnates. The simulation suggests that fast heating initiates the fusion reaction, which produces the measurable neutrons. The result that the heating pulse effectively transport its energy to the core plasma, is promising for promoting the laser fusion scheme. Using the similar Fast Ignition configuration, we showed the roadmap to the power plant.

[1] J. Coutant *et al.*, *Energy from Inertial Fusion, Ch. 5. Inertial fusion energy development strategy* (edited by W.J. Hogan, IAEA, Vienna, Austria, 1995).
[2] W.J. Hogan, *Energy from Inertial Fusion, Ch. 3. IFE Power Plant Design Principles* (edited by W.J. Hogan, IAEA, Vienna, Austria, 1995).
[3] Y. Kitagawa *et al.*, Phys. Rev. Lett. **108**, 155001 (2012).
[4] Y. Kitagawa *et al.*, Plasma Fusion Res. **6**, 1306006 (2011).
[5] T. Kurita *et al.*, Trans. IEE Japan C, Electronics Information and Systems **128**(5), 707 (2008).
[6] A. Sunahara *et al.*, Plasma Fusion Res. **3**, 043 (2008).
[7] Y. Kitagawa *et al.*, Phys. Rev. E **71**, 016403 (2005).
[8] Y. Sentoku *et al.*, Phys. Plasmas **11**, 3083 (2004).